Journal of Virology

Virology | Full-Length Text

Biochemical analysis of the host factor activity of ZCCHC14 in hepatitis A virus replication

You Li,[1] **Stanley M. Lemon**[2,3,4]

AUTHOR AFFILIATIONS See affiliation list on p. 11.

ABSTRACT Relatively little is known of the mechanisms underlying hepatitis A virus (HAV) genome replication. Unlike other well-studied picornaviruses, HAV RNA replication requires the zinc finger protein ZCCHC14 and non-canonical TENT4 poly(A) polymerases with which it forms a complex. The ZCCHC14–TENT4 complex binds to a stem-loop located within the internal ribosome entry site (IRES) in the 5′ untranslated RNA (5′UTR) and is essential for viral RNA synthesis, but the underlying mechanism is unknown. Here, we describe how different ZCCHC14 domains contribute to its RNA-binding, TENT4-binding, and HAV host factor activities. We show that the RNA-binding activity of ZCCHC14 requires both a sterile alpha motif (SAM) and a downstream unstructured domain (D4) and that ZCCHC14 contains two TENT4-binding sites: one at the N-terminus and the other around D4. Both RNA-binding and TENT4-binding are required for HAV host factor activity of ZCCHC14. We also demonstrate that the location of the ZCCHC14-binding site within the 5′UTR is critical for its function. Our study provides a novel insight into the function of ZCCHC14 and helps elucidate the mechanism of the ZCCHC14–TENT4 complex in HAV replication.

IMPORTANCE The zinc finger protein ZCCHC14 is an essential host factor for both hepatitis A virus (HAV) and hepatitis B virus (HBV). It recruits the non-canonical TENT4 poly(A) polymerases to viral RNAs and most likely also a subset of cellular mRNAs. Little is known about the details of these interactions. We show here the functional domains of ZCCHC14 that are involved in binding to HAV RNA and interactions with TENT4 and describe previously unrecognized peptide sequences that are critical for the HAV host factor activity of ZCCHC14. Our study advances the understanding of the ZCCHC14–TENT4 complex and how it functions in regulating viral and cellular RNAs.

KEYWORDS hepatitis A virus, noncanonical poly(A) polymerase, RNA-binding proteins, zinc finger proteins

Hepatitis A virus (HAV) is a positive-strand RNA virus classified in the *Hepatovirus* genus within the Picornaviridae family. It is distinct from other well-studied human picornaviruses in its phylogeny, structure and replication strategy (1, 2). The virus is highly hepatotropic and infects the liver in a stealth-like manner, with the newly replicated virus released from the liver through the biliary tract (3, 4). HAV is noncytopathic, and the acute liver injury that results from infection is due to both adaptive and innate immune responses (5–9). Newly replicated viral progeny are released from infected hepatocytes as quasi-enveloped virions, in which the capsid is cloaked in membranes (10, 11). High concentrations of bile salts disrupt membranous vesicles, leading to shedding of canonical 'naked' viruses in feces (4). Despite good vaccines, the virus remains a common cause of enterically transmitted hepatitis in many countries, with resurgent community outbreaks causing large numbers of hospitalizations in the United States in recent years.

Editor J.-H. James Ou, University of Southern California, Los Angeles, California, USA

Address correspondence to You Li, you_li@med.unc.edu.

The authors declare no conflict of interest.

See the funding table on p. 11.

Received 9 January 2024
Accepted 1 March 2024
Published 19 March 2024

The human terminal nucleotide transferase 4 (TENT4) paralogs, TENT4A and TENT4B, are noncanonical poly(A) polymerases with relaxed nucleotide substrate preferences that extend and incorporate occasional non-adenosine bases into the 3′ poly(A) tails of celluar mRNA (12). Well-conserved among mammals, they form a "TRAMP complex" with the zinc finger CCHC-domain containing protein 7 (ZCCHC7) and the exosome RNA helicase MTR4 in the nucleus that polyadenylates tRNAs, rRNAs, snRNAs, and snoRNAs, thereby regulating nuclear RNA processing and decay (12). In the cytoplasm, TENT4A/B functions redundantly in a TRAMP-like complex involving a different zinc finger protein, ZCCHC14, that catalyzes mixed 3′ tailing, incorporating occasional guanines in poly(A) tails that impede mRNA degradation by deadenylases (13). Hepatitis B virus (HBV) and human cytomegalovirus (HCMV) exploit the ZCCHC14–TENT4 complex to extend poly(A) tails on viral mRNAs that enhance their stability (14–16). Depletion of ZCCHC14 or TENT4A/B suppresses HBV replication and expression of its envelope protein, HBsAg (15), in cell culture. RG7834, a small-molecule inhibitor of TENT4A/B enzymatic activity, potently suppresses HBV replication both *in vitro* and *in vivo* (16, 17). Recently, TENT4-responsive RNA elements have also been found in norovirus, kobuvirus, and saffold virus (18), although the importance of these elements to the replication of these viruses is yet to be determined.

Surprisingly, genome-wide CRISPR screens for HAV host factors have found the ZCCHC14–TENT4 complex to be essential for HAV replication (19, 20). Targeted knockout of ZCCHC14 or TENT4 proteins in hepatoma cells blocks HAV replication, and RG7834 possesses potent anti-HAV activity both in cell culture and in murine models of hepatitis A (20, 21). However, unlike its activity against HBV, inhibiting TENT4 with RG7834 does not reduce the length of the HAV poly(A) tail, suggesting a distinct antiviral mechanism of action (21). We have shown that ZCCHC14 binds to a small stem-loop, SL-Vb, within the 5′ untranslated RNA (5′UTR) of HAV, to which it recruits TENT4 (21). This ZCCHC14–TENT4 complex is required for efficient viral RNA synthesis. Although located within the viral internal ribosome entry site (IRES), the presence or absence of the complex has no impact on HAV protein synthesis (21). The precise function of ZCCHC14–TENT4 in viral RNA synthesis is yet to be determined.

ZCCHC14 is a key adapter protein that bridges TENT4 with its target RNAs: HAV, HBV, HCMV, and possibly others. It contains a sterile alpha motif (SAM) (Fig. 1A), which may be an RNA-binding domain (22) but has not been validated experimentally. ZCCHC14 is a large protein (1,086 amino acids), and the functions of the SAM motif and other domains within the protein have not been studied. Here, we describe an analysis of ZCCHC14 and the function of its different domains in RNA-binding, TENT4-binding, and HAV replication. Our results reveal a previously unrecognized domain (D4) that is important for both RNA-binding and TENT4-binding activities of ZCCHC14 and the surprising presence of two distinct TENT4-binding sites within ZCCHC14: one at the N-terminus and the other adjacent to D4. Both RNA-binding and TENT4-binding activities are required for optimal HAV host factor activity of ZCCHC14. In addition, we demonstrate that the position within the genome to which ZCCHC14 recruits TENT4 is critical, as SL-Vb, the stem-loop that binds ZCCHC14, fails to support viral replication when moved from the 5′UTR to a position downstream within the genome. Our study helps understand the functions of ZCCHC14–TENT4 in regulation of the RNA transcripts of HAV and other relevant viruses, as well as cellular RNAs targeted by the complex.

RESULTS

ZCCHC14 domains required for RNA-binding activity

The structure of the ZCCHC14 protein is unknown. The AlphaFold 2.0 program (https://alphafold.ebi.ac.uk/) predicts five structural domains (D1–D5) separated by disordered regions within ZCCHC14 (Fig. 1B and C). D3 corresponds to the SAM motif, a putative RNA-binding domain, whereas D5 contains the zinc knuckle motif (ZnK). The D2 domain shares homology with a phosphoinositide (PI)-binding module, whereas D1 and D4 have no homology to known protein structures. The prediction confidence is high for D1–D3,

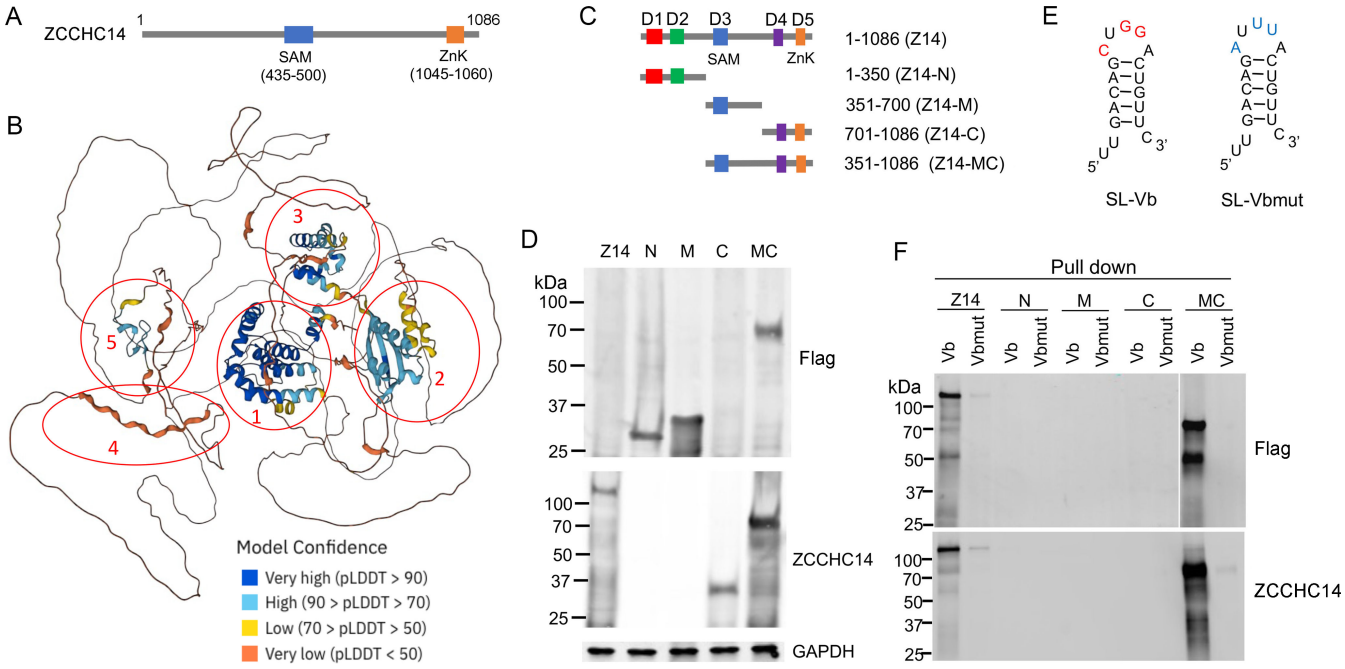

FIG 1 (A) Linear sequence of ZCCHC14 showing the position of the SAM motif and zinc knuckle (ZnK) (B) Structure of human ZCCHC14 predicted by AlphaFold 2.0. Putative structural domains are numbered from 1 to 5, with model confidence coded by colors. (C) Diagram depicting the full-length ZCCHC14 and different fragment constructs. (D) Immunoblots of 293T cell lysates transfected with indicated constructs with Flag (*upper*) or ZCCHC14 (*lower*) antibodies. (E) Structure of the HAV stem-loop (SL) Vb (nts 644–661) and loop mutant (Vbmut) RNAs. (F) Pulldown of indicated ZCCHC14 constructs with a 3′ biotinylated synthetic RNA probe representing SL Vb and Vb-mut, blotted with Flag (*upper*) or ZCCHC14 (*lower*) antibodies.

moderate for D5, and relatively low for D4, suggesting that D4 may be unstructured under physiological conditions or only structured within a protein complex. To define the function of these different ZCCHC14 domains, we constructed plasmids expressing different FLAG-tagged fragments of ZCCHC14 (Fig. 1C), including an N-terminal fragment (Z14-N, aa 1–350, D1 +D2), a middle fragment containing the SAM domain (Z14-M, aa 351–700, D3), and C-terminal fragment containing the ZnK motif (Z14-C, aa 701–1,086, D4 +D5). An additional construct spanned the SAM and ZnK motifs (Z14-MC, aa 351–1,086, D3 +D4+D5). These constructs were FLAG-tagged at the N-terminus, as was the full-length ZCCHC14 (Z14), and were expressed as expected in 293T cells (Fig. 1D). The Z14-C fragment was not efficiently detected by the FLAG antibody, likely due to the instability of the amino-terminus of this fragment, but was readily detected by the ZCCHC14 antibody, which recognizes the carboxy-terminal ZnK domain (Fig. 1D, bottom panel).

To test the ability of these different ZCCHC14 fragments to bind RNA corresponding to the SL-Vb stem-loop, we used an RNA pulldown assay described previously (21). Briefly, a 3′ biotin-labeled synthetic SL-Vb RNA probe was incubated with lysates of 293T cells transfected with these expression vectors. Proteins binding the probe were isolated on streptavidin beads and assayed for FLAG and ZCCHC14 by immunoblotting. As a negative control for these experiments, we used a mutant SL-Vb probe with a loop sequence altered to remove the CNGGN motif required for ZCCHC14 binding (Fig. 1E) (21). Surprisingly, none of the Z14-N, Z14-M, or Z14-C fragments bound SL-Vb (Fig. 1F), even though Z14-M contains the SAM motif, a putative RNA-binding domain. This was not due to degradation of the fragments during the assay as the fragments were readily detected in the residual post-pulldown material (Fig. S1A). Only Z14-MC could bind SL-Vb (Fig. 1F), indicating that the sequence outside the D3 SAM domain is required for the specific SL-Vb RNA-binding activity of ZCCHC14.

To better define the requirements for RNA binding, we deleted amino acids 648–814 between the D3 SAM and D4 domains in Z14-MC (MCΔ648–814) (Fig. 2A). This construct

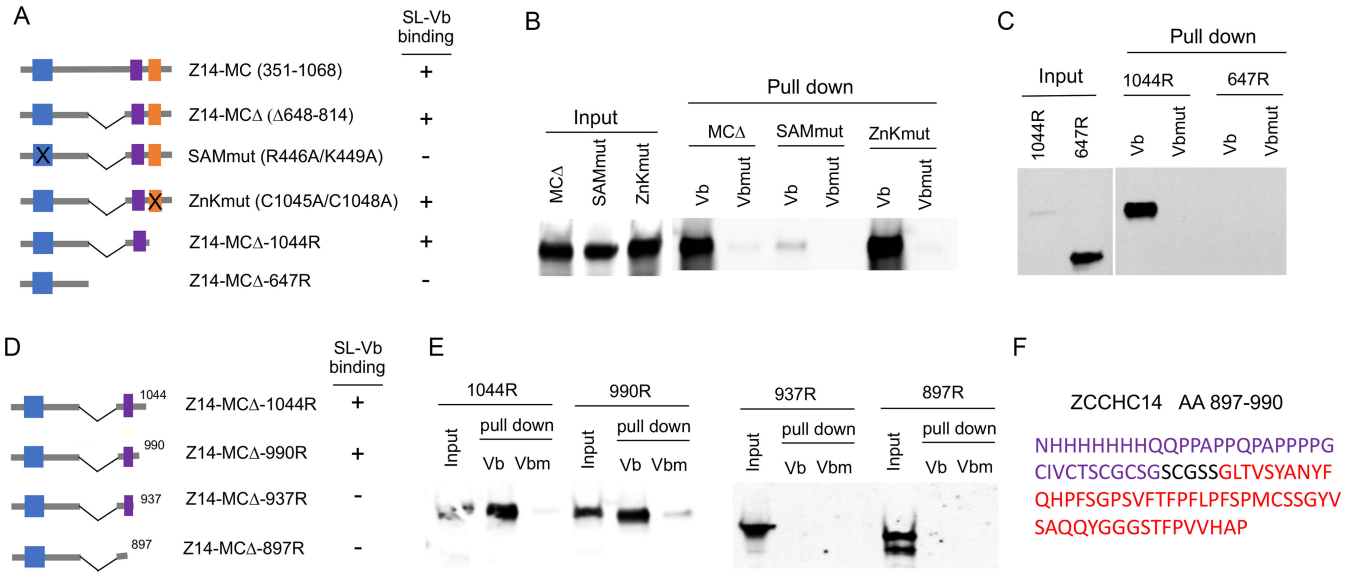

FIG 2 (A) Diagram depicting the different mutations/deletions made to the Z14-MC construct and their SL-Vb binding activities. (B) and (C) RNA pulldown assay as in Fig. 1F with indicated ZCCHC14 constructs in (A). (D) Diagram depicting constructs with deletions around D4 and their SL-Vb binding activities. (E) RNA pulldown assay as in Fig. 1F with indicated constructs in (D). (F) Sequence of the predicted D4 structure (Fig. 1B, purple) and its downstream disordered region (red) required for SL-Vb binding. All blots are carried out with the Flag antibody.

preserved SL-Vb binding (Fig. 2B; Fig. S1B). The SAM domain contains a conserved RLHKY motif (aa 446–450 in ZCCHC14) that is considered to be critical for RNA-binding activity (22). We mutated these arginine and lysine residues to alanine in the Z14-MCΔ fragment (SAMmut) (Fig. 2A). This resulted in a substantial loss of RNA binding (Fig. 2B) without affecting the stability of the protein (Fig. S1C), confirming that the SAM motif is indeed necessary, but not sufficient for SL-Vb binding. The ZnK motif contains conserved CCHC residues. We mutated the first two Cs (C1045 and C1048 in ZCCHC14) to alanine in Z14-MCΔ648–814 (ZnKmut) (Fig. 2A). The ZnKmut fragment readily bound SL-Vb (Fig. 2B), indicating that the zinc finger motif is not required for RNA binding. Consistent with this, a complete deletion of ZnK did not affect SL-Vb binding (Z14-MCΔ−1044R) (Fig. 2A and C). By contrast, extending the C-terminal deletion to include D4 resulted in a complete loss of SL-Vb binding (Z14-MCΔ−647R) (Fig. 2A and C), indicating that the region around D4 is essential for the RNA-binding activity of ZCCHC14. To further dissect the region around D4, we made additional deletions between D4 and the ZnK motif (Fig. 2D). While deleting amino acids 990–1,044 (990R) had no effect on SL-Vb pulldown, deleting amino acids 937–990 (937R) completely abolished RNA-binding activity (Fig. 2E). This sequence corresponds to a segment of the protein that is predicted to be disordered immediately downstream of D4 (Fig. 2F). A larger deletion involving D4 (897R) also led to a loss of RNA-binding activity (Fig. 2E). Taken collectively, these data show that the stem-loop Vb binding activity of ZCCHC14 requires both the SAM motif in D3 and a disordered segment of the protein downstream of D4.

ZCCHC14 contains two TENT4-binding sites

Next, we tested the ability of the different ZCCHC14 fragments to associate with TENT4 proteins using a co-immunoprecipitation (co-IP) assay. For this purpose, 293T lysates expressing HA-tagged ZCCHC14 fragments were incubated with purified recombinant FLAG-tagged TENT4 protein fragments (aa 226–558 of TENT4A or aa 186–518 of TENT4B) representing the catalytic domains of these noncanonical polymerases (kindly provided by Arbutus Biopharma) or a bovine serum albumin (BSA) control and immunoprecipitated with anti-FLAG magnetic beads. We focused on the catalytic domains because the full-length TENT4 proteins are relatively large (80–90 kD) and not readily

amenable to bacterial expression and purification. Immunoprecipitants were blotted with the FLAG antibody to detect TENT4 proteins and the HA antibody to detect the ZCCHC14 fragments. As anticipated, full-length ZCCHC14 protein co-precipitated with both TENT4A and TENT4B (Fig. 3A). Surprisingly, however, both the Z14-N and Z14-C fragments were pulled down by TENT4 (Fig. 3B), whereas Z14-M was not. Both of these interactions appear to be RNA-independent, as neither was abolished by pretreating the lysates with RNase 1 (Fig. 3C). These data suggest the surprising conclusion that there are two discrete TENT4-binding sites within ZCCHC14. We made further deletions in the Z14-N and Z14-C fragments to assess the ability of individual domains (D1, D2, D4, and ZnK) to bind TENT4. These results suggest that peptide sequences around D1 (Fig. 3D) and D4 (Fig. 3E) are important for TENT4 binding. Interestingly, the same disordered region that is required for RNA binding (aa 937–990) is also required for TENT4 binding. A partial deletion of this sequence (fragment aa 701–937) (Fig. 3E) substantially reduced the interaction with TENT4, which was completely abolished by further deletion of D4 (fragment aa 701–897) (Fig. 3E).

The HAV host factor activity of ZCCHC14 requires both RNA and TENT4 binding

We next assessed the capacity of the different ZCCHC14 constructs to support HAV replication. We depleted endogenous ZCCHC14 in 293T cells by transfecting specific siRNAs and then reconstituted the expression of the protein by transfecting vectors expressing the different ZCCHC14 fragments. The cells were then infected with HAV/18f-NLuc recombinant virus, which expresses nanoluciferase as a reporter (19). Luciferase activities were measured at 48 or 72 hours post-infection as an indication of HAV replication. As expected, the expression of Z14-N, Z14-M, and Z14-C fragments did not rescue HAV replication in ZCCHC14-depleted cells (Fig. 4A and B). Alanine substitutions within the SAM motif abolished the capacity of ZCCHC14 to support HAV replication (Fig. 4C), consistent with its role in binding SL-Vb. In contrast, ablating the ZnK motif had no effect on the ability of ZCCHC14 to support replication (Fig. 4C). Expression of the Z14-MC fragment partially restored HAV replication (Fig. 4C), suggesting that the

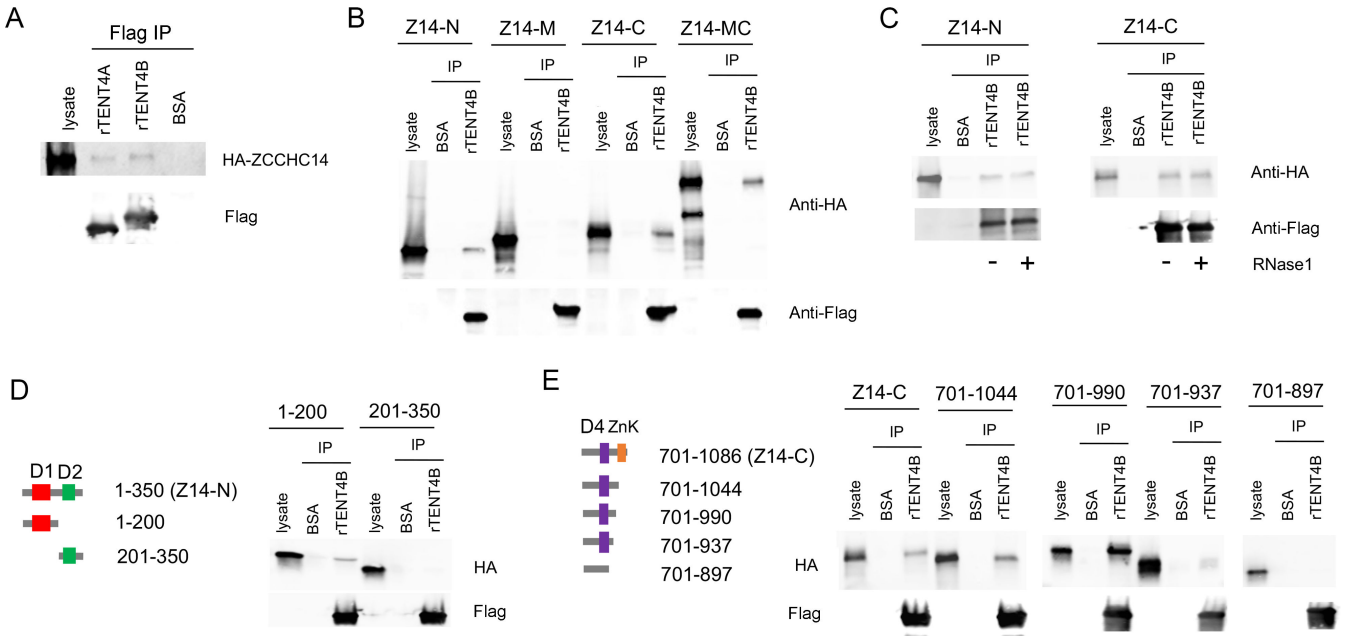

FIG 3 (A) Immunoprecipitation of 293T lysate expressing HA-ZCCHC14 with purified recombinant FLAG-TENT4A or FLAG-TENT4B proteins. BSA is used as a negative control. (B) IP as in (A) with indicated ZCCHC14 constructs. (C) IP as in (B) with RNase 1 treatment. (D) (*left*) Diagram depicting deletions made in the Z14-N fragment and (*right*) their interaction with TENT4 in the co-IP assay. (E) (*left*) Diagram depicting deletions made in the Z14-C fragment and (*right*) their interaction with TENT4 in the co-IP assay.

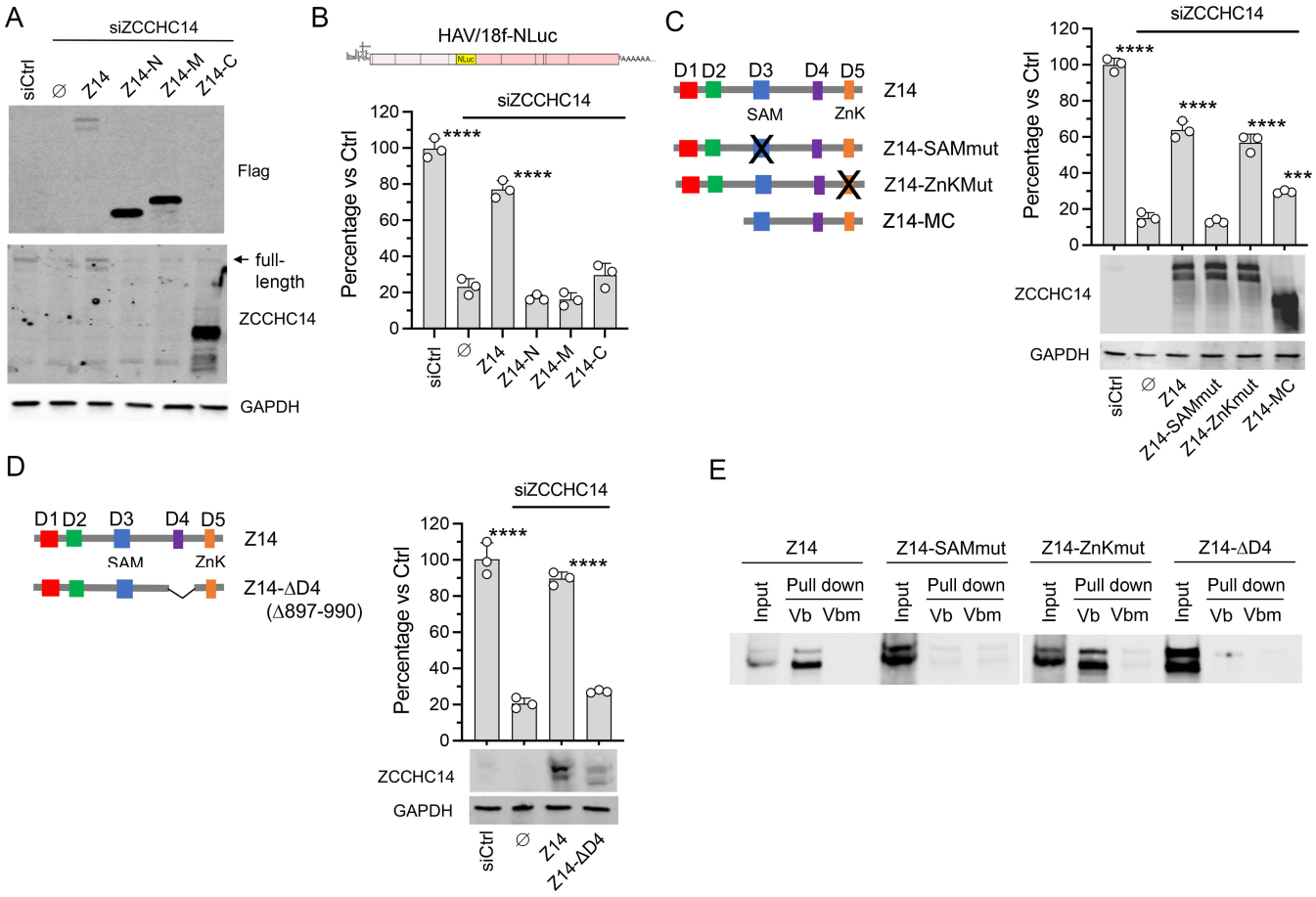

FIG 4 (A) Immunoblots of ZCCHC14-depleted 293T cells expressing indicated FLAG-ZCCHC14 constructs with Flag (*upper*) or ZCCHC14 (*lower*) antibodies. The arrow denotes the full-length ZCCHC14 protein. (B) (*upper*) Organization of the HAV 18f-NLuc reporter virus genome and (*lower*) NLuc expression 48 hrs following 18f-NLuc infection of ZCCHC14-depleted 293T cells with and without the overexpression of indicated ZCCHC14 constructs. Data representative of three experiments, each with three technical replicates. ****P < 0.001 relative to the mock reconstituted sample (ø). (C) (*left*) Diagram depicting the mutations/deletions made to the ZCCHC14 construct. (*right*) NLuc expression 48 hours following 18f-NLuc infection and immunoblots of ZCCHC14-depleted 293T cells with and without the overexpression of indicated ZCCHC14 constructs. Data representative of two experiments, each with three technical replicates. ***P < 0.005, ****P < 0.001 relative to the mock reconstituted sample (ø). (D) (*left*) Diagram depicting the D4 deletion construct. (*right*) NLuc expression 48 hours following 18f-NLuc infection and immunoblots of ZCCHC14-depleted 293T cells with and without overexpression of indicated ZCCHC14 constructs. Data representative of two experiments, each with three technical replicates. ****P < 0.001 relative to the mock reconstituted sample (ø). (E) SL-Vb RNA pulldown assay as in Fig. 1F with indicated mutations/deletions made within the full-length ZCCHC14 construct. Blot was with ZCCHC14 antibody.

N-terminal region of ZCCHC14, which contains one of the TENT4-binding sites, is needed for optimal host factor activity. As expected, deleting the region around D4 (aa 897–990, Z14-ΔD4) resulted in a complete loss of host factor activity (Fig. 4D). We confirmed that mutationally ablating the SAM domain and deleting D4 in the full-length ZCCHC14 protein abolished binding to SL-Vb (Fig. 4E), consistent with results described previously in experiments with truncated versions of the protein (Fig. 2). By contrast, ablating the ZnK domain had no effect on SL-Vb binding. Importantly, none of these mutations promoted degradation of the protein (Fig. S1D).

SL-Vb function in HAV replication is position-dependent

The SL-Vb sequence is highly conserved among different HAV strains and contains a penta-nucleotide loop sequence motif matching ZCCHC14-binding stem-loops in HBV and human cytomegalovirus (HCMV) mRNAs (14, 21). CLIP-seq experiments have identified SL-Vb as the major site of ZCCHC14 binding within the HAV genome (21).

The stem-loop is located within the IRES, but studies done years ago demonstrated that it is not required for HAV IRES activity (23, 24), whereas other studies show that it is critical for optimal replication of the HAV genome (21). It is not known whether the location of SL-Vb within 5′UTR is critical for its function in replication or whether it could function like the *cis*-acting replication element (*cre*) stem-loop in a position-independent fashion (25). To better understand this, we relocated SL-Vb from the 5′UTR to a position near the center of the genome in a replication-competent virus. To accomplish this, we mutated the SL-Vb sequence in the 18f-NLuc reporter virus (Vbmut) (Fig. 5A) so that it no longer binds ZCCHC14 or optimally supports replication (Fig. 1E, F and 5B) (21). We then inserted the SL-Vb structure at the junction of the NLuc reporter and 2B sequences in Vb-mut, in frame with the polyprotein sequence, to determine whether this would recover replication (Vbmut-Vb) (Fig. 5A). We tested the replication competence of these viral RNAs, together with a viral RNA containing both the authentic SL-Vb and a second copy of SL-Vb inserted between NLuc and 2B (Vb-Vb), by monitoring nanoluciferase expression after transfection into Huh-7.5 cells (Fig. 5B). Insertin of the stem-loop sequence at the NLuc-2B junction (Vb-Vb) did not affect replication, indicating that the insertion is well-tolerated. However, while the mutation of the authentic SL-Vb (Vbmut) reduced HAV replication more than twofold, the downstream insertion of SL-Vb (Vbmut-Vb) did not rescue virus replication. The infectious virus yields from these RNAs were consistent with their replication levels (Fig. 5C). The relatively small difference in replication capacity (about two fold) resulting from the deletion of SL-Vb in Vb-mut is likely due to residual binding of ZCCHC14 to the 5′UTR upstream of SL-Vb (Fig. 5D). While our previously published CLIP-seq data (21) suggest SL-Vb is the primary ZCCHC14-binding site, nucleotides upstream of SL-Vb (nts 169–598) also bind ZCCHC14, albeit with lower efficiency (Fig. 5D). Taken collectively, these data indicate that SL-Vb is required for optimal recruitment of ZCCHC14 to the 5′UTR and suggest furthermore that the position of SL-Vb within the genome is critical for its function.

DISCUSSION

Despite being a well-established host factor for HAV and HBV replication, little is known about the structure of the zinc finger RNA-binding protein, ZCCHC14. ZCCHC14 is known to bridge TENT4 polymerases with their target RNAs (14, 21), but the details of this interaction are also unclear. Here, we have used an AlphaFold predicted structure to analyze the different putative domains of ZCCHC14 and their roles in RNA binding, TENT4 interaction, and HAV host factor activity. Our results reveal that the peptide sequence near a previously unrecognized ZCCHC14 domain, D4 (Fig. 1B), is important for both RNA binding and TENT4 interaction. This region is predicted to be unstructured by AlphaFold2. Its sequence is rich in serines and glycines (Fig. 2F), which are considered disorder-promoting amino acids. The serine-rich nature of the domain suggests this region may contain phosphorylation sites, but there is no evidence of phosphorylation in the PhosphoSitePlus database. Our functional assays confirm this region is critical for supporting HAV replication (Fig. 4D).

In addition to classic globular RNA-binding domains, like RNA-recognition motifs (RRM) and K-homology domain (KH), emerging evidence suggests that intrinsically disordered regions (IDRs) may also contribute to RNA-binding activities (26). For example, the flexible linker regions in the poly(A)-binding protein (PABP) and polypyrimidine tract binding protein 1 (PTBP1) facilitate RNA-binding activity (27, 28). RNA-binding proteins may contain disordered regions along with well-defined RNA-binding domains, such as the SAM motif and D4 in ZCCHC14. The disordered regions can enhance the RNA-binding specificity and affinity by providing additional contact points and facilitating dynamic interactions (26). How the disordered region in D4 facilitates ZCCHC14 binding to the HAV SL-Vb RNA is unknown. One caveat of the biochemical studies with ZCCHC14 fragments is that large truncations may disrupt the folding of protein domains. In this regard, it is possible that the D4 region is involved in maintaining the folding of the SAM domain, rather than direct RNA binding. Further structural studies

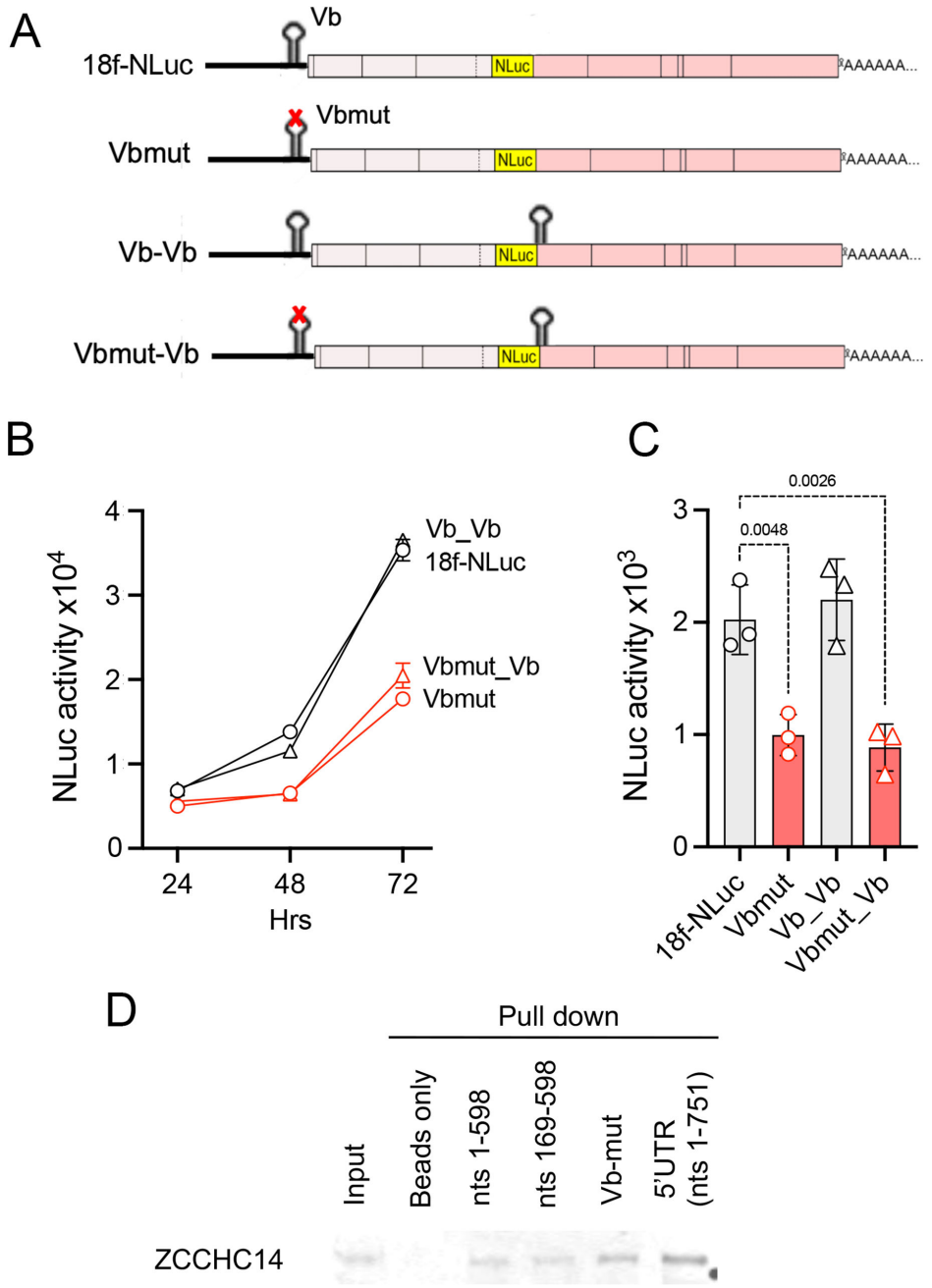

FIG 5 (A) Diagram depicting the SL-Vb mutation/insertion made to the 18f-NLuc virus genome. (B) RNAs made from the constructs in (A) were transfected into Huh7.5 cells, and luciferase activities were measured at 24, 48, and 72 hrs to determine the levels of HAV replication. (C) Cell culture supernatants from (B) were collected at 72 hrs post-transfection and used to re-infect Huh7.5 cells. Luciferase activities were measured at 48 hrs post-infection. Data representative of two experiments, each with three technical replicates. (D) Pulldown of endogenous ZCCHC14 in the Huh7.5 lysate with 3′ biotinylated RNA probes representing HAV 5′UTR (nts 1–751), 5′UTR with mutated SL-Vb (Vb-mut), and upstream sequences (nts 1–598 and nts 169–598), blotted with the ZCCHC14 antibody.

with ZCCHC14 bound to its target RNAs are needed to elucidate the detail of this interaction.

Several different adapter proteins have been identified for TENT4 polymerases, including ZCCHC7, ZCCHC14, and ZCCHC2, all of which recruit TENT4 to different RNA targets. In the nucleus, ZCCHC7 interacts with TENT4 to form the classic "TRAMP

complex" that polyadenylates tRNAs, rRNAs, snRNAs, and snoRNAs (12). ZCCHC2 is a recently identified TENT4 adapter protein that binds to distinct RNA motifs (18). ZCCHC7 binds the TENT4 protein through its zinc finger domains (29, 30), while the zinc finger domain of ZCCHC2 is implicated in RNA binding (18). Surprisingly, the zinc finger domain in ZCCHC14, ZnK, (Fig. 1A) is not required for either RNA binding or TENT4 interaction (Fig. 2B and 3E) and is moreover dispensable for HAV replication (Fig. 4C). ZCCHC2 interacts with TENT4 through its N-terminal domain (18). Interestingly, the N-terminal domains of ZCCHC2 and ZCCHC14 share high sequence similarity (18). This is consistent with our data indicating that the N-terminal domain of ZCCHC14, D1 (Fig. 3D) binds TENT4 and is required for the optimal host factor activity of ZCCHC14 in HAV replication (Fig. 4C). However, it is curious that the disordered region in D4 also forms a complex with TENT4 (Fig. 3E). Given the highly flexible and dynamic property of IDRs, it is not uncommon for them to enable proteins to interact with a wide range of binding partners, and they often undergo induced conformational change upon binding to specific proteins (31). Our observation that ZCCHC14 contains two TENT4-binding sites is based on *in vitro* biochemical assays with ZCCHC14 fragments. It is unknown whether *in vivo* these two sites function separately or alternatively fold together to form one master TENT4 interaction site. Given the fact that D4 participates in both RNA binding and TENT4 interaction, it is tempting to think that upon binding to its target RNA, D4 may undergo conformational change that promotes TENT4 interaction, or *vice versa*, that binding of TENT4 to D4 facilitates RNA-binding activity.

HAV, like other picornaviruses, possesses a "*cis*-acting replication element," or *cre*, within the $3D^{pol}$ coding sequence that is essential for uridylation of VPg, a viral protein that functions as the primer for viral RNA synthesis (25, 32, 33). The *cre* folds into a stem-loop structure with two conserved adenines in the loop segment that template the uridylation reaction (25, 34). The function of the *cre* is position-independent: it remains functional when placed at alternative positions within the genome (25). In contrast, the function of SL-Vb, the binding site of ZCCHC14, is position-dependent: when SL-Vb is inserted at the junction of the NLuc reporter and 2B sequence, it is incapable of supporting HAV replication (Fig. 5). This result suggests the location of SL-Vb, and thus the binding of ZCCHC14 to the 5'UTR is critical. It is suprsing that the mutation of SL-Vb resulted in only moderate reduction (two to three fold) of viral replication, in contrast to ZCCHC14 knockout, which nearly completely blocks replication (21). One possible explanation is that accessory ZCCHC14 binding outside SL-Vb can partially support replication when the high-affinity binding site SL-Vb is absent. This is consistent with our data showing that the sequence upstream of SL-Vb (nts 169–598) can bind ZCCHC14 at reduced efficiency (Fig. 5D). There is no SL-Vb-like motif within this upstream region, and the specific sequences/motifs that confer this supplementary ZCCHC14 binding remain to be determined.

TENT4 proteins, as 3' polyadenylases, are known to recognize the 3' ends of RNAs (35). The apparent importance of ZCCHC14 binding to 5'UTR is consistent with a model we have previously proposed (21) in which the ZCCHC14–TENT4 complex forms a protein bridge between 5' and 3' ends of HAV RNA to functionally circularize the genome, with ZCCHC14 binding near the 5' end of the genome and TENT4 interacting with the 3' UTR. This hypothesis is attractive because genome circularization has been demonstrated to be important for other (+)-strand RNA viruses, including poliovirus, which like HAV, is a picornavirus (36, 37). Circularization of the poliovirus genome is mediated by PCBP2 and the viral 3 CD protein bound to a 5' cloverleaf-like structure interacting with poly(A)-binding protein (PABP) bound to the 3' poly(A) tail (37). This enables the 3Dpol polymerase to position itself at the 3' end of (+)-RNA for (-)-strand initiation. HAV could adopt a similar strategy to initiate (-)-strand RNA synthesis using the ZCCHC14–TENT4 complex. Although speculative, this hypothesis would provide a step in viral RNA synthesis that has yet to be demonstrated for HAV but is known to be required for other picornaviruses.

MATERIALS AND METHODS

Cells and viruses

293T and human liver-derived Huh-7.5 cells were obtained from ATCC and Apath LLC, respectively. The cell culture-adapted HAV variant HM175/18 f and its nanoluciferase (NLuc) reporter virus derivative, 18f-NLuc, have been described previously (19).

Plasmids

Various ZCCHC14 fragments were generated by PCR with specific primers with a 5′BamHI site and 3′ NotI site and inserted into pcDNA3–FLAG or pCK–HA vector for the expression of FLAG- or HA-tagged proteins. Mutations in SAM or ZnK domains were introduced by the QuikChange Site-Directed Mutagenesis kit (Agilent, #200523). Plasmid expressing deletion of D4 (Z14-ΔD4) was constructed by inserting the commercially synthesized DNA fragment into the BsrGI and MluI sites of the full-length ZCCHC14 plasmid.

Transfection

Plasmid transfection was carried out with Trans-IT LT1 reagent (Mirus Bio, # MIR 2304) following the manufacturer's instruction. Viral RNAs were transfected with the Trans-IT mRNA reagent (Mirus Bio, # MIR 2225). siRNA pools targeting ZCCHC14(L-014086–01) and a control (siCtrl) siRNA pool were purchased from Horizon Discovery. siRNAs were transfected into cells with Lipofectamine RNAiMax reagent (Thermo Fisher, 13778075) at a final concentration of 20 nM.

Western blot

Approximately 10^6 Huh-7.5 or 293T cells were lysed in radioimmunoprecipitation assay (RIPA) buffer (20–188, Millipore) for 20 min on ice and clarified by centrifugation at 14,000 g for 10 min at 4°C. The lysate was mixed with 4 × Laemmli buffer, incubated at 95°C for 5 min, and resolved in a 4–15% gradient SDS–polyacrylamide pre-cast gel (4561086, BioRad). Proteins were transferred to a polyvinylidene fluoride membrane by semi-dry transfer using the Trans-Blot Turbo apparatus (BioRad). Membranes were blocked in Odyssey Blocking Buffer (LI-COR Biosciences) and probed with a 1:1,000 dilution of primary antibodies overnight. The membrane was washed with 0.05% Tween-20 and probed with a 1:10,000 dilution of donkey anti-goat secondary antibodies conjugated with IRDye 800 or IRDye 680 (LI-COR Biosciences) for 1 h at room temperature. Excess secondary antibodies were removed by washing with 0.05% Tween-20, and protein bands were visualized using an Odyssey Infrared Imaging System (LI-COR Biosciences). The following antibodies were used: ZCCHC14 rabbit polyclonal antibody (Bethyl Labs, A303-096A), mouse monoclonal antibody to FLAG (Cell Signaling Technology #8146), rabbit polyclonal antibody to GAPDH (Proteintech, 10494–1-AP), and goat polyclonal antibody to HA (Fortis Life, A190-138A).

Biotinylated RNA pulldown

3′ biotinylated HAV SL-Vb and SL-Vb mutant RNAs were commercially synthesized by Integrated DNA Technology. Ten pmol of biotinylated RNAs was heated at 75°C for 5 min and then cooled to room temperature. The annealed RNA baits were bound to magnetic streptavidin T1 beads (Thermo Fisher, #65601) following the manufacturer's protocol and then incubated with the 293T cytoplasmic lysate overnight at 4°C. Proteins bound to the beads were washed four times with PBS with 1% Triton and eluted with SDS-PAGE sample buffer.

Co-immunoprecipitation

293T cells expressing HA-ZCCHC14 constructs were harvested in lysis buffer [150 mM KCl, 25 mM Tris-HCl pH 7.4, 5 mM EDTA, 1% Triton X-100, 5 mM DTT, complete protease

inhibitor cocktail (Roche)]. Lysates were centrifuged, and supernatants were incubated with 1 ug of purified FLAG-TENT4A, TENT4B, or BSA control at 4°C for 2 h, followed by addition of 30 uL of magnetic anti-FLAG beads (Millipore #M8823) for 1 h. The beads were washed four times in lysis buffer and eluted with SDS-PAGE sample buffer.

Luciferase reporter assay

Cells infected with 18f-NLuc virus were lysed in 1 × passive lysis buffer (Promega) for 15 min at room temperature. Cell lysates were transferred to an opaque white 96-well plate (Corning, 3912). Nluc assays were carried out with the Nluc GLOW Assay kit (Nanolight Technology, #325). Luminescence was measured using a Biotek Synergy II multi-mode plate reader (BioTek Instruments).

Statistical analysis

Statistical analysis was carried out with Prism 10 software using one-way ANOVA with correction for multiple comparisons; *P*-values were adjusted by the FDR method.

ACKNOWLEDGMENTS

The authors gratefully acknowledge the technical assistance of Bryan Yonish.

This work was supported in part by grants from the National Institute of Allergy and Infectious Diseases of the U.S. National Institutes of Health: R21-AI163606, R41-AI177204 (YL), R01-AI150095, and R01-AI103083 (SML).

AUTHOR AFFILIATIONS

[1]Department of Pediatrics, University of North Carolina at Chapel Hill, Chapel Hill, North Carolina, USA
[2]Department of Medicine, The University of North Carolina at Chapel Hill, Chapel Hill, North Carolina, USA
[3]Department of Microbiology & Immunology, The University of North Carolina at Chapel Hill, Chapel Hill, North Carolina, USA
[4]Lineberger Comprehensive Cancer Center, The University of North Carolina at Chapel Hill, Chapel Hill, North Carolina, USA

AUTHOR ORCIDs

You Li http://orcid.org/0000-0001-5458-6009
Stanley M. Lemon http://orcid.org/0000-0003-1450-806X

FUNDING

Funder	Grant(s)	Author(s)
HHS | NIH | National Institute of Allergy and Infectious Diseases (NIAID)	R21-AI163606, R41-AI177204	You Li
HHS | NIH | National Institute of Allergy and Infectious Diseases (NIAID)	R01-AI150095, R01-AI103083	Stanley M. Lemon

AUTHOR CONTRIBUTIONS

You Li, Conceptualization, Data curation, Formal analysis, Funding acquisition, Investigation, Methodology, Project administration, Writing – original draft, Writing – review and editing | Stanley M. Lemon, Funding acquisition, Resources, Writing – review and editing

DATA AVAILABILITY

The authors confirm that the data supporting the findings of this study are available within the article and its supplementary materials.

ADDITIONAL FILES

The following material is available online.

Supplemental Material

Fig. S1 (JVI00057-24-s0001.docx). Immunoblots.

REFERENCES

1. McKnight KL, Lemon SM. 2018. Hepatitis A virus genome organization and replication strategy. Cold Spring Harb Perspect Med 8:a033480. https://doi.org/10.1101/cshperspect.a033480
2. Smith DB, Simmonds P. 2018. Classification and genomic diversity of enterically transmitted hepatitis viruses. Cold Spring Harb Perspect Med 8:a031880. https://doi.org/10.1101/cshperspect.a031880
3. Lanford RE, Feng Z, Chavez D, Guerra B, Brasky KM, Zhou Y, Yamane D, Perelson AS, Walker CM, Lemon SM. 2011. Acute hepatitis A virus infection is associated with a limited type I interferon response and persistence of intrahepatic viral RNA. Proc Natl Acad Sci U S A 108:11223–11228. https://doi.org/10.1073/pnas.1101939108
4. Hirai-Yuki A, Hensley L, Whitmire JK, Lemon SM. 2016. Biliary secretion of quasi-enveloped human hepatitis A virus. mBio 7:e01998-16. https://doi.org/10.1128/mBio.01998-16
5. Hirai-Yuki A, Hensley L, McGivern DR, González-López O, Das A, Feng H, Sun L, Wilson JE, Hu F, Feng Z, Lovell W, Misumi I, Ting J-Y, Montgomery S, Cullen J, Whitmire JK, Lemon SM. 2016. MAVS-dependent host species range and pathogenicity of human hepatitis A virus. Science 353:1541–1545. https://doi.org/10.1126/science.aaf8325
6. Walker CM, Feng Z, Lemon SM. 2015. Reassessing immune control of hepatitis A virus. Curr Opin Virol 11:7–13. https://doi.org/10.1016/j.coviro.2015.01.003
7. Sun L, Li Y, Misumi I, González-López O, Hensley L, Cullen JM, McGivern DR, Matsuda M, Suzuki R, Sen GC, Hirai-Yuki A, Whitmire JK, Lemon SM. 2021. IRF3-mediated pathogenicity in a murine model of human hepatitis A. PLoS Pathog 17:e1009960. https://doi.org/10.1371/journal.ppat.1009960
8. Misumi I, Mitchell JE, Lund MM, Cullen JM, Lemon SM, Whitmire JK. 2021. T cells protect against hepatitis A virus infection and limit infection-induced liver injury. J Hepatol 75:1323–1334. https://doi.org/10.1016/j.jhep.2021.07.019
9. Sung PS, Hong S-H, Lee J, Park S-H, Yoon SK, Chung WJ, Shin E-C. 2017. CXCL10 is produced in hepatitis A virus-infected cells in an IRF3-dependent but IFN-independent manner. Sci Rep 7:6387. https://doi.org/10.1038/s41598-017-06784-x
10. Feng Z, Hensley L, McKnight KL, Hu F, Madden V, Ping L, Jeong S-H, Walker C, Lanford RE, Lemon SM. 2013. A pathogenic picornavirus acquires an envelope by hijacking cellular membranes. Nature 496:367–371. https://doi.org/10.1038/nature12029
11. Das A, Rivera-Serrano EE, Yin X, Walker CM, Feng Z, Lemon SM. 2023. Cell entry and release of quasi-enveloped human hepatitis viruses. Nat Rev Microbiol 21:573–589. https://doi.org/10.1038/s41579-023-00889-z
12. Yu S, Kim VN. 2020. A tale of non-canonical tails: gene regulation by post-transcriptional RNA tailing. Nat Rev Mol Cell Biol 21:542–556. https://doi.org/10.1038/s41580-020-0246-8
13. Lim J, Kim D, Lee Y-S, Ha M, Lee M, Yeo J, Chang H, Song J, Ahn K, Kim VN. 2018. Mixed tailing by TENT4A and TENT4B shields mRNA from rapid deadenylation. Science 361:701–704. https://doi.org/10.1126/science.aam5794
14. Kim D, Lee Y-S, Jung S-J, Yeo J, Seo JJ, Lee Y-Y, Lim J, Chang H, Song J, Yang J, Kim J-S, Jung G, Ahn K, Kim VN. 2020. Viral hijacking of the TENT4-ZCCHC14 complex protects viral RNAs via mixed tailing. Nat Struct Mol Biol 27:581–588. https://doi.org/10.1038/s41594-020-0427-3
15. Hyrina A, Jones C, Chen D, Clarkson S, Cochran N, Feucht P, Hoffman G, Lindeman A, Russ C, Sigoillot F, Tsang T, Uehara K, Xie L, Ganem D, Holdorf M. 2019. A genome-wide CRISPR screen identifies ZCCHC14 as a host factor required for hepatitis B surface antigen production. Cell Rep 29:2970–2978. https://doi.org/10.1016/j.celrep.2019.10.113
16. Mueller H, Lopez A, Tropberger P, Wildum S, Schmaler J, Pedersen L, Han X, Wang Y, Ottosen S, Yang S, Young JAT, Javanbakht H. 2019. PAPD5/7 are host factors that are required for hepatitis B virus RNA stabilization. Hepatology 69:1398–1411. https://doi.org/10.1002/hep.30329
17. Mueller H, Wildum S, Luangsay S, Walther J, Lopez A, Tropberger P, Ottaviani G, Lu W, Parrott NJ, Zhang JD, Schmucki R, Racek T, Hoflack J-C, Kueng E, Point F, Zhou X, Steiner G, Lütgehetmann M, Rapp G, Volz T, Dandri M, Yang S, Young JAT, Javanbakht H. 2018. A novel orally available small molecule that inhibits hepatitis B virus expression. J Hepatol 68:412–420. https://doi.org/10.1016/j.jhep.2017.10.014
18. Seo JJ, Jung SJ, Yang J, Choi DE, Kim VN. 2023. Functional viromic screens uncover regulatory RNA elements. Cell 186:3291–3306. https://doi.org/10.1016/j.cell.2023.06.007
19. Das A, Barrientos R, Shiota T, Madigan V, Misumi I, McKnight KL, Sun L, Li Z, Meganck RM, Li Y, Kaluzna E, Asokan A, Whitmire JK, Kapustina M, Zhang Q, Lemon SM. 2020. Gangliosides are essential endosomal receptors for quasi-enveloped and naked hepatitis A virus. Nat Microbiol 5:1069–1078. https://doi.org/10.1038/s41564-020-0727-8
20. Kulsuptrakul J, Wang R, Meyers NL, Ott M, Puschnik AS. 2021. A genome-wide CRISPR screen identifies UFMylation and TRAMP-like complexes as host factors required for hepatitis A virus infection. Cell Rep 34:108859. https://doi.org/10.1016/j.celrep.2021.108859
21. Li Y, Misumi I, Shiota T, Sun L, Lenarcic EM, Kim H, Shirasaki T, Hertel-Wulff A, Tibbs T, Mitchell JE, McKnight KL, Cameron CE, Moorman NJ, McGivern DR, Cullen JM, Whitmire JK, Lemon SM. 2022. The ZCCHC14/TENT4 complex is required for hepatitis A virus RNA synthesis. Proc Natl Acad Sci U S A 119:e2204511119. https://doi.org/10.1073/pnas.2204511119
22. Aviv T, Lin Z, Lau S, Rendl LM, Sicheri F, Smibert CA. 2003. The RNA-binding SAM domain of Smaug defines a new family of post-transcriptional regulators. Nat Struct Biol 10:614–621. https://doi.org/10.1038/nsb956
23. Brown EA, Zajac AJ, Lemon SM. 1994. *In vitro* characterization of an internal ribosomal entry site (IRES) present within the 5' nontranslated region of hepatitis A virus RNA: comparison with the IRES of encephalomyocarditis virus. J Virol 68:1066–1074. https://doi.org/10.1128/JVI.68.2.1066-1074.1994
24. Brown EA, Day SP, Jansen RW, Lemon SM. 1991. The 5' nontranslated region of hepatitis A virus RNA: secondary structure and elements required for translation *in vitro*. J Virol 65:5828–5838. https://doi.org/10.1128/JVI.65.11.5828-5838.1991
25. Yang Y, Yi M, Evans DJ, Simmonds P, Lemon SM. 2008. Identification of a conserved RNA replication element (*cre*) within the $3D^{pol}$-coding sequence of hepatoviruses. J Virol 82:10118–10128. https://doi.org/10.1128/JVI.00787-08
26. Järvelin AI, Noerenberg M, Davis I, Castello A. 2016. The new (dis)order in RNA regulation. Cell Commun Signal 14:9. https://doi.org/10.1186/s12964-016-0132-3
27. Oberstrass FC, Auweter SD, Erat M, Hargous Y, Henning A, Wenter P, Reymond L, Amir-Ahmady B, Pitsch S, Black DL, Allain F-T. 2005. Structure of PTB bound to RNA: specific binding and implications for splicing regulation. Science 309:2054–2057. https://doi.org/10.1126/science.1114066
28. Deo RC, Bonanno JB, Sonenberg N, Burley SK. 1999. Recognition of polyadenylate RNA by the poly(A)-binding protein. Cell 98:835–845. https://doi.org/10.1016/s0092-8674(00)81517-2
29. Fasken MB, Leung SW, Banerjee A, Kodani MO, Chavez R, Bowman EA, Purohit MK, Rubinson ME, Rubinson EH, Corbett AH. 2011. Air1 zinc knuckles 4 and 5 and a conserved IWRXY motif are critical for the function and integrity of the Trf4/5-Air1/2-Mtr4 polyadenylation (TRAMP) RNA quality control complex. J Biol Chem 286:37429–37445. https://doi.org/10.1074/jbc.M111.271494

30. Hamill S, Wolin SL, Reinisch KM. 2010. Structure and function of the polymerase core of TRAMP, a RNA surveillance complex. Proc Natl Acad Sci U S A 107:15045–15050. https://doi.org/10.1073/pnas.1003505107
31. Holehouse AS, Kragelund BB. 2024. The molecular basis for cellular function of intrinsically disordered protein regions. Nat Rev Mol Cell Biol 25:187–211. https://doi.org/10.1038/s41580-023-00673-0
32. Paul AV, Rieder E, Kim DW, van Boom JH, Wimmer E. 2000. Identification of an RNA hairpin in poliovirus RNA that serves as the primary template in the *in vitro* uridylylation of VPg. J Virol 74:10359–10370. https://doi.org/10.1128/jvi.74.22.10359-10370.2000
33. McKnight KL, Lemon SM. 1998. The rhinovirus type 14 genome contains an internally located RNA structure that is required for viral replication. RNA 4:1569–1584. https://doi.org/10.1017/s1355838298981006
34. Paul AV, Yin J, Mugavero J, Rieder E, Liu Y, Wimmer E. 2003. A "slide-back" mechanism for the initiation of protein-primed RNA synthesis by the RNA polymerase of poliovirus. J Biol Chem 278:43951–43960. https://doi.org/10.1074/jbc.M307441200
35. Rammelt C, Bilen B, Zavolan M, Keller W. 2011. PAPD5, a noncanonical poly(A) polymerase with an unusual RNA-binding motif. RNA 17:1737–1746. https://doi.org/10.1261/rna.2787011
36. Villordo SM, Gamarnik AV. 2009. Genome cyclization as strategy for flavivirus RNA replication. Virus Res 139:230–239. https://doi.org/10.1016/j.virusres.2008.07.016
37. Herold J, Andino R. 2001. Poliovirus RNA replication requires genome circularization through a protein-protein bridge. Mol Cell 7:581–591. https://doi.org/10.1016/s1097-2765(01)00205-2